



Single-side polished lithium niobate SAW wafers

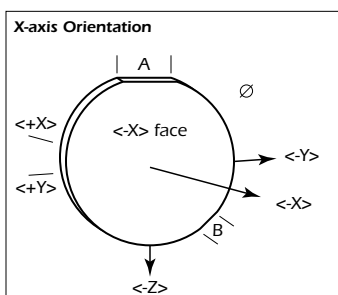
Applications

- Surface Acoustic Wave Devices
- Optical Wave Guides
- Optical Low Pass Filters
- Optical Isolators
- Wollaston Prisms



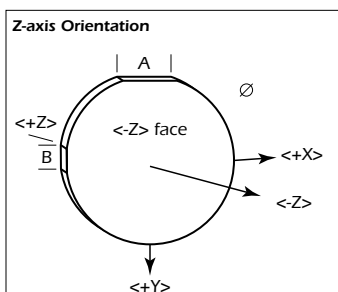
Double-side polished lithium niobate optical wafers

Lithium Niobate Wafers — Optical



Orientation: X-axis (all dimensions in mm)

Part #	A	B	Thickness	Ø	-X / +X
97-01183-01	20.3	14.0	0.5	76.2	polished / ground
99-00629-01	20.3	14.0	0.5	76.2	polished / polished
97-00663-01	20.3	14.0	1.0	76.2	polished / ground
99-00630-01	20.3	14.0	1.0	76.2	polished / polished
97-01912-01	30.5	15.2	1.0	100	polished / ground
97-01763-10	30.5	15.2	1.0	100	polished / polished
97-02604-01	42.5	27.5	1.0	125	polished / polished



Orientation: Z-axis (all dimensions in mm)

Part #	A	B	Thickness	Ø	-Z / +Z
97-00567-03	20.3	14.0	0.5	76.2	polished / ground
99-00042-01	20.3	14.0	0.5	76.2	polished / polished
97-00567-01	20.3	14.0	1.0	76.2	polished / ground
99-60011-01	20.3	14.0	1.0	76.2	polished / polished
97-01514-10	30.5	15.2	1.0	100	polished / polished
97-02641-01	42.5	27.5	1.0	125	polished / polished

Lithium Niobate Single Crystal Substrate

Basic Overview

The following discussion answers common questions customers have when processing lithium niobate single crystal substrates for a variety of applications.

- Handling
- Cleaning
- Surface Quality
- Wafer Flatness
- Crystal Polarity

Scratch #	Max width (μ)	Dig #	Max diameter (μ)
10	1	5	50
20	2	10	100
40	4	20	200
60	6	40	400

Table 1. Scratch-Dig

Handling

As is the case with most substrate materials used in device manufacture, operators should take the precautions of using gloves and vacuum wands when handling LN substrates. The plastic shipping containers, either individual carriers or boats of up to 25 wafers, should be sealed at all times and opened only under a flow hood or in a clean-room environment. In addition to these considerations, there are a few properties specific to LN of which all personnel involved in its handling should be aware.

- 1) LN is a brittle material. Our edge-grinding process minimizes chipping and cracking by producing a smooth radius on the wafer's edge. For other product geometries, edge bevels serve the same function. However, care must still be taken to avoid rough handling or impact of any kind to LN substrates. Vacuum wands or tweezers should ideally be made of relatively soft, non-metallic materials. This also applies to any carriers or boats used in wafer processing equipment.
- 2) LN is both pyroelectric and piezoelectric, and therefore generates an electrical potential when either thermally cycled or mechanically stressed. Since thermal cycling is virtually unavoidable during device manufacturing, it is important to be aware of the effects of these properties. Most importantly, build-up of static charge on the wafer causes it to act as a 'dust magnet'. Hence, special care must be taken to maintain a particulate-free environment during and after thermal processing. The charge build-up may also create mechanical strains in the crystal, and thereby increase the risk of wafer breakage. Thermal shock should be avoided by allowing for gradual heating and cooling ramps (as a rule of thumb, we recommend ~1 degree Celsius/minute). In routine processing the piezoelectric properties of LN shouldn't present a problem, as long as the wafer is not squeezed excessively in fixturing or during handling.

Cleaning

In standard volume wafer production, CTI uses either cassette-to-cassette automated wafer scrubbing or sonic batch cleaning.

For routine hand-cleaning of parts, we recommend immersion in a solution of soapy water with a pH between 7.0 and 8.5 or low concentration ammonia in water, followed by hand-wiping with undenatured ethyl alcohol, or, in a mixture of four parts alcohol and one part acetone. Using a litho-pad, lens tissue, or cotton swab, the hand-wiping should always occur in a continuous motion from one edge to the other to avoid leading- or trailing-edge stains.

Throughout any cleaning process, manual or otherwise, it is critical to avoid letting the wafer dry during intermediary steps or prior to the final drying step. Premature drying leaves stains or residue from the baths or cleaning solutions that can be difficult to remove. Parts should be moved directly from bath to bath and should not sit out in open air prior to the final drying step, whether that is spin-drying, vapor degreasing, or manual blow-drying.

Surface Quality

The U.S. Military Surface Quality Specification, MIL-O-13830A, is a standard for the specification of surface quality in optical components. This standard is used at CTI to specify various levels of surface quality in our products, and is commonly referred to as 'scratch-dig'. We compare our products with scratch and dig standards manufactured according to U.S. military drawing C7641866 Rev L, and our inspection areas are equipped with lighting which meets the standard's requirements.

In the scratch-dig system, a given quality level is expressed as two numbers—the first specifies the maximum allowable width of scratches, and the second specifies the maximum allowable diameter of digs, or pits. Typical scratch-dig numbers used at CTI range from 10-5 to 60-40, and specify defect size limits as shown in Table 1.

Wafer Flatness

Flatness is a critical parameter in many applications for LN wafers, particularly those involving the photolithography of fine structures (<1 micron). CTI employs a non-contact, grazing incidence interferometer to analyze reflected fringe patterns and reconstruct the wafer topography mathematically. Because of the oblique angle of incidence of the laser source, the machine is capable of measuring as-cut or lapped surfaces as well as polished surfaces.

Wafers can be sorted by a variety of flatness parameters, both clamped (using a vacuum chuck) and unclamped (free-state). Clamped parameters include total indicated reading (TIR), total thickness variation (TTV), and taper. Unclamped parameters include warp and bow. The figure below provides definitions for each of these.

For standard wafers, CTI specifies clamped wafer flatness by TTV alone. This also allows customers the opportunity to verify flatness on wafers using a digital micrometer and the five point measurement method for gauging total thickness variation as described in ASTM standard F533. For specifying free-state flatness in standard wafers, warp alone is used, since the bow parameter as defined here is primarily used to describe the direction of curvature, not the overall magnitude.

Flatness on the surfaces of non-wafer geometry's of LN (blocks, plates) are measured with an interferometer. Flatness is expressed in fraction of the wavelength of the incident light, 633 nm.

Crystal Polarity

Many LN applications call for the specification of electrical polarity of the various faces of the fabricated substrate. Upon heating or compression of lithium niobate across the c axis, the lithium and niobium ions move closer to their centered (paraelectric) positions relative to the oxygen layers of the unit cell. This reduced net polarization allows a compensating buildup of electrons on the plus face, causing it to become negatively charged.

Accordingly, LN polarity is determined by measuring the charge generated from heating or squeezing a part with a micro-voltmeter. The deflection of the needle (positive or negative) indicates the polarity of a given face. In practice, we have found that heating the crystal, as opposed to squeezing it, provides the least ambiguous result and the least potential for damaging polished surfaces.

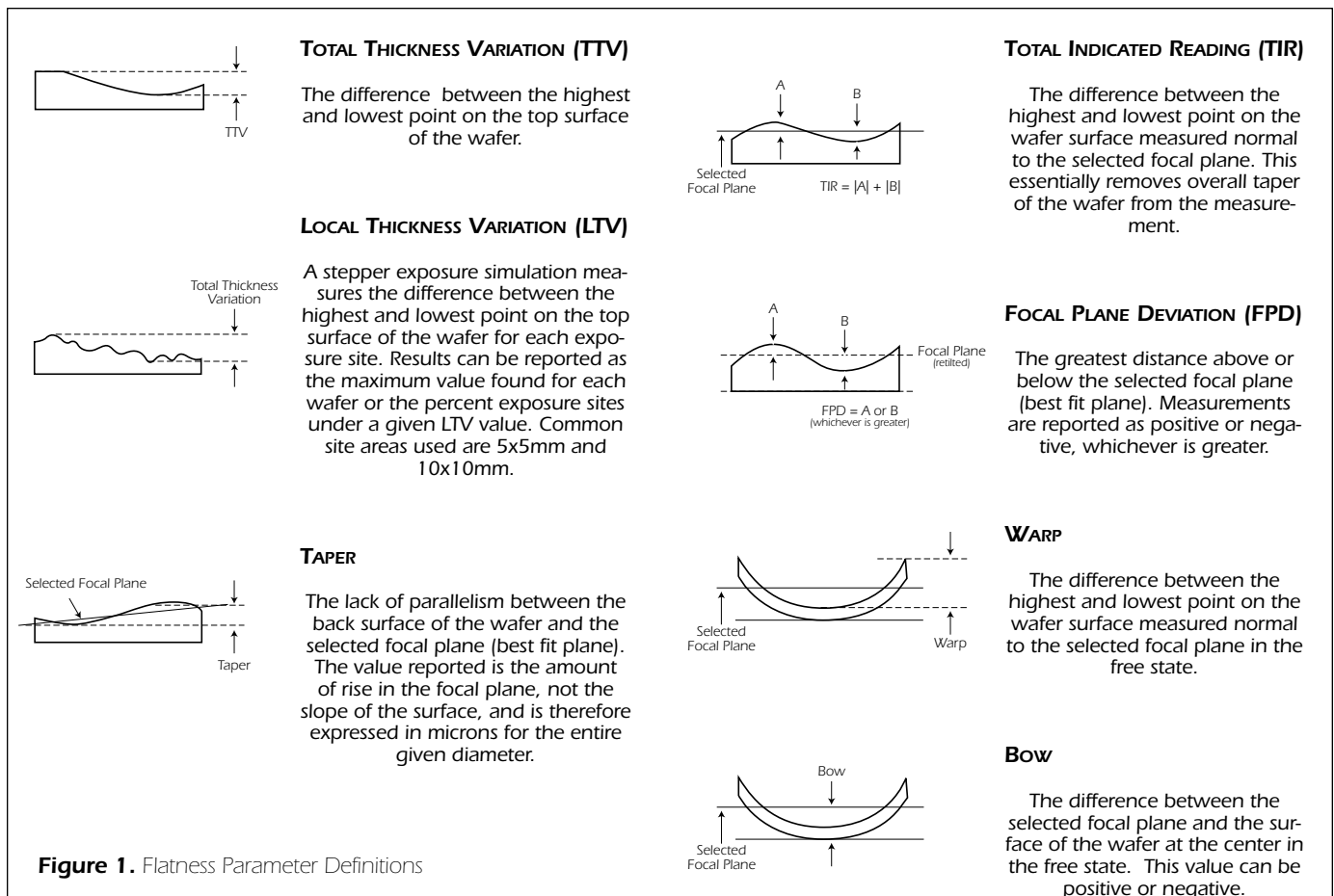


Figure 1. Flatness Parameter Definitions

Black Lithium Niobate

Chemically Reduced Lithium Niobate: Processing, Properties and Improvements in SAW Device Fabrication and Performance

Lithium niobate (LN) single crystals find wide application as substrates for surface acoustic wave (SAW) devices. This material's large piezoelectric coefficients enable fabrication of SAW filters with low insertion loss. The optical transparency and pyroelectric response of LN may, however, cause problems in its processing and application.

The high pyroelectric constant makes LN susceptible to charging upon undergoing temperature changes. These surface charges can spontaneously short, with the associated sparking causing processing or operational failures. Common processes such as photoresist baking or wire bonding can induce such discharges. For finished SAW devices, discharges due to changes in ambient temperature can produce undesired voltage spikes as seen in Figure 1.

Reduction processing generally is applied to LN after growth and poling. The degree of reduction depends on the reduction temperature and gas atmosphere, as well as the crystal's surface roughness, Li/Nb composition and sample size. For these experiments, lapped 128° RY LN wafers of congruent composition were reduced in an atmosphere of 10% H₂ and 90% N₂ for one hour at temperatures ranging from 400°C to 750°C. After reduction, wafers were polished on both sides and analyzed electrically and optically.

To test reduced LN wafers' susceptibility to pyroelectric charging, wafers were cooled on a hot plate from 120°C to 80°C at 10°C/min. while the surface charge was monitored using an electric field meter. For untreated LN wafers such a procedure typically generates a surface field of 2 kV/cm, which requires several hours to dissipate. As shown in Figure 2, none of the reduced wafers showed any measurable electric field.

SAW filters with a center frequency of 78 MHz were fabricated at Andersen Laboratories from several reduced as well as untreated wafers. Center frequency, insertion loss, SAW velocity and temperature coefficient of reduced LN were the same as untreated LN under normal operating conditions.

We gratefully acknowledge Ray Sawin and Jeff Galipeau of Andersen Laboratories for fabrication and testing of the SAW samples.

References:

Bordui, P.F. et al., J. Appl. Phys., (1999), 85(7): p. 3766-3769.

Standifer, E.M. et. al., Proceedings of the 1998 International Frequency Control Symposium. (1998).

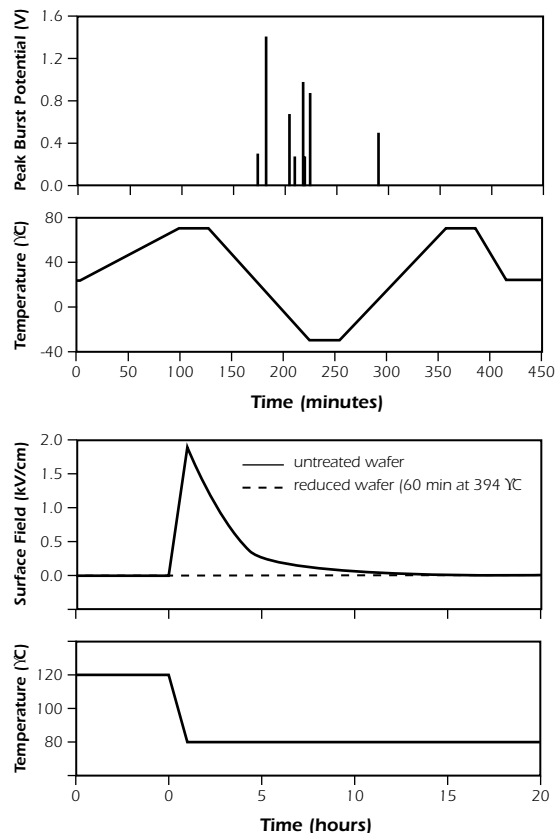


Figure 1. Pyroelectric test results for SAW devices fabricated on untreated LN. The lower graph shows the temperature ramp used for the test. The upper graph shows the peak burst voltages for the observed pyroelectric discharges. Eight bursts were detected. On treated LN, no bursts were observed.

Figure 2. Surface electric field upon cooling such as is typical during processing. Solid line: untreated LN. Dashed line: LN reduced at 394°C for 1 hr.

Lithium Niobate Material Quality Classification

Crystal Technology, Inc. currently specifies three grades of crystal quality. As a general rule, crystal quality is continuously improved as the processes are improved. However, there are often trade-offs between improving quality and reducing costs. Our technical staff regularly meets with the leading customers in each industry in order to find the best compromise between quality improvements and cost reduction. The following material grades are in order from the least critical (and lowest cost) to the most demanding:

- SAW Grade
- Refractive Grade
- Optical Grade

SAW Grade

This is the most commonly produced grade and is used for making surface acoustic wave devices. This is a non-optical applications and the least demanding in terms of impurities and crystalline perfection. Reduced material ("black LN") is often adequate or even preferred for its lack of pyro-electric charging. Inclusions can be tolerated to some extent as long as they are small enough not to interfere with the excitation or propagation of the SAW waves. Crystal growth for SAW material is generally optimized for high efficiency. The crystals are grown quite long, converting a large fraction of the melt into crystal material.

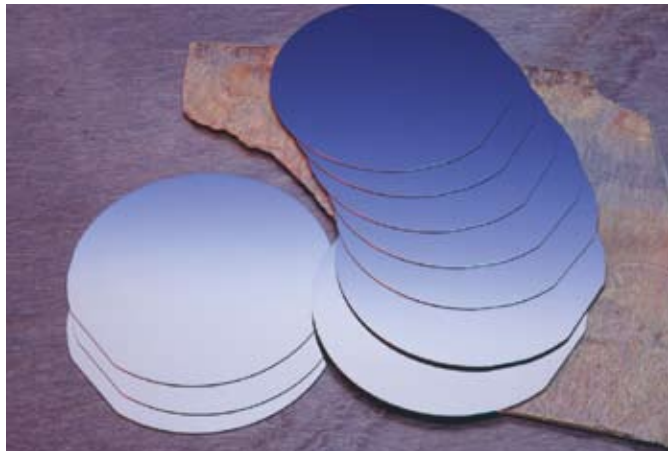
CTI rejects material that is excessively colored (excessive contamination), cracked, or shows signs of twinning or large angle grain boundaries ($>0.2^\circ$). Material with large inclusions or a high density of smaller inclusions is also rejected.

Refractive Grade

This is material used for lower demanding optical applications such as Wollaston prisms for DVD heads and blur-filters for digital still cameras. Strain (dislocations) are tolerable, but inclusions are not. The crystals are grown at similar lengths to SAW grade material, but inspected and screened to avoid even low densities of inclusions.

Optical Grade

This material is used for the most demanding optical applications such as high speed modulators and polarization-controlling devices. Optical material is low strain with no inclusions. To avoid grain boundaries and strain build-up, the crystals are grown shorter (typically less than half the SAW grade crystal length). The growth environment (furnace construction) as well as growth parameters (pull rate, rotation) are optimized for low strain, not high throughput. To minimize effects of non-congruency and impurities, a smaller fraction of the melt (~50%) is converted into crystal than for the other two grades. A proprietary inspection method is used to visualize strain before the crystal is sliced. Only the best of these crystals are further processed, with the others either graded as refractive or recycled.



Chemically reduced (black) lithium niobate SAW wafers.

Periodically Poled Lithium Niobate (PPLN)

PPLN crystals offer high gain and non-critical quasi phase-matching for a wide range of nonlinear optical interactions, such as difference frequency generation and OPO applications pumped in the near infrared. In addition to single grating devices, where only one interaction is phase-matched, PPLN chips with multiple gratings along the propagation direction, chirped gratings, and fan-out gratings are also feasible.

PPLN devices offered by Crystal Technology are fabricated from our integrated optics substrates using electrical field poling process, and meet stringent criteria for uniformity and crystalline quality. The most popular PPLN part numbers for DFG and OPO applications have various periodicity patterns on the same chip. This enables coarse tuning by translating the chip so that a different grating is utilized. Fine tuning is achieved by adjusting the temperature of the PPLN device. The period required for phase-matching a particular interaction is easily calculated and Figure 1 shows the example of an OPO pumped by a Nd:YAG or Ti:Sapphire laser with output wavelengths ranging from 1.5µm to 4µm.

- | Applications | |
|--------------|---|
| ■ | High resolution mid IR spectroscopy |
| ■ | OPO and DFG for laser science experiments |
| ■ | Missile counter-measure laser systems |

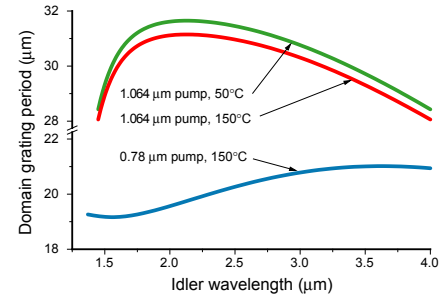


Figure 1. Grating periods required for OPO operation in PPLN

Sellmeier Equation for n_e in Congruent LN	Parameter & Value
$f = (T - 24.5^\circ\text{C}) / (T + 570.82)$	$a_1 = 5.35583$ $b_1 = 4.629 \times 10^{-7}$
$n_e^2 = a_1 + b_1 f + \frac{a_2 + b_2 f}{\lambda^2 - (a_3 + b_3 f)^2} + \frac{a_4 + b_4 f}{\lambda^2 - a_5^2} - a_6 \lambda^2$	$a_2 = 0.100473$ $b_2 = 3.862 \times 10^{-8}$
	$a_3 = 0.20692$ $b_3 = -0.89 \times 10^{-8}$
	$a_4 = 100$ $b_4 = 2.657 \times 10^{-5}$
	$a_5 = 11.34927$
	$a_6 = 0.015334$
	$\lambda = \text{wavelength in } \mu\text{m}$

Domain Periods (µm)								Y (mm)	Z (mm)	X (mm)	Part #		
25.5	25.9	26.4	26.9	27.4	27.8	28.2	28.7	11.5	0.5	20	97-02182-06		
								11.5	1	20	97-02384-06		
								11.5	0.5	50	97-02182-08		
								11.5	1	50	97-02384-08		
28.5	28.7	28.9	29.1	29.3	29.5	29.7	29.9	11.5	0.5	20	97-02182-03		
								11.5	1	20	97-02384-03		
								11.5	0.5	50	97-02182-07		
								11.5	1	50	97-02384-07		
30.0	30.2	30.4	30.6	30.8	30.95	31.1	31.2	11.5	0.5	20	97-02256-01		
								11.5	1	20	97-02383-01		
								11.5	0.5	50	97-02256-02		
								11.5	1	50	97-02383-02		
18.6	18.8	19.0	19.2	19.4	19.6	19.8	20.0	20.2	20.4	11.5	0.5	20	97-02355-01



PPLN substrate has been etched to reveal domain strips.



Magnesium-doped Periodically Poled Lithium Niobate (MgO:PPLN)

MgO PPLN material has successfully been used to generate green¹ and blue² laser beams with good efficiency. Crystal Technology produces a range of such crystals where all the critical manufacturing steps are performed in house. Our growth method is well developed and geared to high volume production thus lowering manufacturing cost and allowing our crystals to be deployed into mass market application such as laser projection displays and other consumer applications. The purity of starting powders and the crystal growth parameters are tightly controlled to ensure consistent quality guaranteeing stable optical properties. Our research has resulted in crystal growth that is guaranteed to avoid photorefractive damage yielding devices with well controlled refractive index and birefringence.

Our proprietary electric-field poling method ensures good domain fidelity leading to high nonlinear effective coefficients and our MgO:PPLN material has successfully been employed to generate green and blue laser beams by frequency-doubling of semiconductor lasers. Figure 1 shows inverted domain patterns in MgO:PPLN. The high fidelity on both the +Z face as well as the opposite crystal face demonstrates the capability and reproducibility of the poling process.

The standard MgO:PPLN parts have 3 periodicities on a chip to allow the user to optimize operating temperature for the device. Figure 2 shows the frequency doubled power of a single-mode laser at 1064nm as a function of the chip temperature for each of the three periods. Both anti-reflection coated as well as uncoated chips are available in three lengths, 1mm, 3mm and 10mm to support both short and long pulsed sources at various power levels. Custom designs are also available.

MgO:PPLN offers unique advantages for frequency doubling to visible wavelengths because it is a non-critical quasi phase-matching interaction utilizing the highest nonlinear optical coefficient d_{33} . A short crystal ensures high conversion efficiency in ultra-short pulse lasers while minimizing group velocity dispersion.³ The large nonlinearity together with a long crystal allows high second harmonic generation efficiencies even at modest power levels. A 10mm long crystal for example will generate over 50mW of green light at circulating fundamental power of less than 4W assuming confocal focusing.

Applications	
■	SHG for green and blue generation from IR sources
■	Laser Based RGB displays

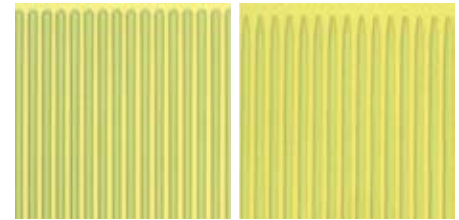


Figure 1. Inverted domain patterns on the two faces of the crystal, demonstrating good fidelity throughout the crystal volume.

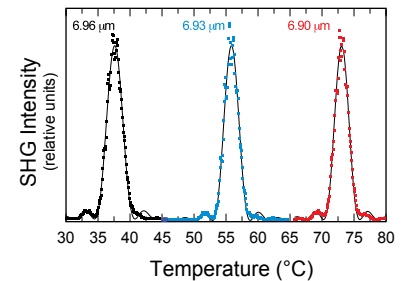


Figure 2. Temperature tuning of 1064nm frequency doubling for three gratings on 10mm chip.

Domain Periods (μm)	Y (mm)	Z (mm)	X (mm)	Part #
6.9 - 6.96 for 1064nm doubling, No AR coating, $d_{\text{eff}} > 14 \text{ pm/V}$	3	0.5	1	97-03040-01
	3	0.5	3	97-03040-02
	3	0.5	10	97-03040-03
6.9 - 6.96 for 1064nm doubling, DAR, $R < 0.25\% @ 1064 \text{ nm}$, $R < 0.5\% @ 532 \text{ nm}$, $d_{\text{eff}} > 14 \text{ pm/V}$	3	0.5	1	97-03038-01
	3	0.5	3	97-03038-02
	3	0.5	10	97-03038-03
5.22 - 5.27 for 976nm doubling, No AR coating, $d_{\text{eff}} > 14 \text{ pm/V}$	3	0.5	1	97-03043-01
	3	0.5	3	97-03043-02
	3	0.5	10	97-03043-03
5.22 - 5.27 for 976nm doubling, DAR, $R < 0.25\% @ 976 \text{ nm}$, $R < 0.5\% @ 488 \text{ nm}$, $d_{\text{eff}} > 14 \text{ pm/V}$	3	0.5	1	97-03042-01
	3	0.5	3	97-03042-02
	3	0.5	10	97-03042-03

REFERENCES

1. H. Furuya, A. Morikawa, K. Mizuuchi, and K. Yamamoto, Jpn. J. Appl. Phys., Part 1 45, 6704 (2006).
2. M. Maiwald, S. Schwertfeger, R. Guther, B. Sumpf, K. Paschke, C. Dzionk, G. Erbert, and G. Trankle, Opt. Lett. 31, 802 (2006).
3. M. A. Arbore and M. M. Fejer, Opt. Lett. 22, 13-15 (1997).

Optical Materials for Visible Light Applications

Magnesium-doped Lithium Niobate

While congruently melting lithium niobate (CLN) can be grown at large size and with excellent uniformity, the material suffers from photorefractive damage.¹ This undesirable effect can be avoided by using magnesium oxide (MgO) doped LN.^{2,3}

Crystal Technology has done extensive research on growth and characterization of MgO:LN.⁴ Dozens of crystals have been grown from various starting melt compositions to establish optimal growth parameters for achieving crystals of high optical quality. The OH absorption peak location is a good indicator of the anti-site defect density. Material with a fully shifted OH absorption peak is “above threshold” and resilient to photorefractive and thus useful for visible light applications. Figure 1 shows absorption spectra of crystal samples with different compositions. Only the sample showing a single, shifted peak (green) would be useful. Based on such results, we have chosen a starting melt composition that guarantees all wafers from the grown crystal to be free of photorefractive. Although it is common to state only the MgO concentration for a photorefractive resistant material, our research confirms that precise control of the Li/Nb ratio is also necessary to guarantee a crystal above threshold.⁵

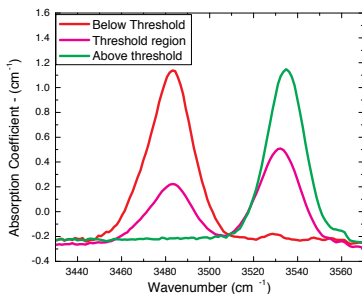


Figure 1. OH absorption peak of 3 slices from the same crystal.

Phase-matching temperature (SHG to 532 nm using d_{32} or d_{33}) is a sensitive characterization tool to reveal axial composition variations and to distinguish crystals grown from different compositions. Such measurements resolve differences as low as 0.04 mol% of MgO in the melt.⁴ Figure 2 shows the results of phase matching temperature as function of solidified melt fraction for crystals grown from different MgO concen-

trations in the melt, ranging from 4.9 to 6.0 mol%. In this range, the phase-matching temperature decreases with increasing MgO concentration. For every grown crystal, the temperature increases with increasing solidified melt fraction, indicating that the magnesium concentration decreases during growth, consistent with a distribution coefficient higher than 1.⁶

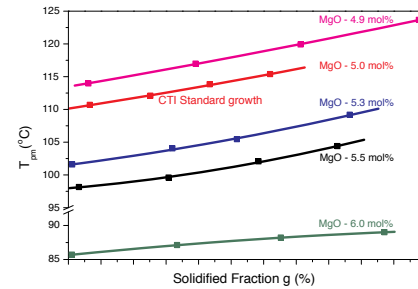


Figure 2. Birefringent Phase-matching temperature as function of solidified melt fraction for different starting melt compositions, including CTI standard composition at MgO 5.0 mol%

The impact of different Li/Nb ratios for the same initial MgO concentration on the phase-matching temperature is smaller, but clearly measurable. While a certain variation from top to bottom of a grown crystal is unavoidable, this effect is controlled in our growths to minimize the impact on the customer's application. The quasi-phase-matching temperature for 1064nm SHG for example varies by less than 4°C for any crystal produced with our standard wafer material.

The growth experiments and precision characterization tools have enabled Crystal Technology to optimize the overall growth process. This allows a lower wafer cost while still maintaining the required performance consistency. All wafers are guaranteed to be from a crystal entirely above the photorefractive threshold, and the birefringent phase-matching temperature for every wafer is between 109 °C and 116 °C.

Stoichiometric Lithium Tantalate (SLT)

Crystal Technology produces 3” diameter SLT wafers by the VTE method. This material has been successfully used for high power generation of visible light.⁷ Photorefractive, GRIIRA,⁸ as well as peak power damage are further reduced as compared to MgO:LN.⁷ CTI started delivery of SLT wafers and PP:SLT devices in 2009.

Materials Research

Crystal Technology is continually expanding the product portfolio for periodically poled devices and wafers used to produce such devices. A recent breakthrough allows production modified CLN with lowered absorption from 2.5µm to 2.8µm, making OPO oscillation possible at these wavelengths. Another example is superoxidized LN which offers improved photorefractive properties over CLN.^{9,10} Scaled-up processes are under development to provide this material at reasonable cost.

Products

To see the latest product offering, please visit our website. Double-side polished Z-axis oriented 3” diameter wafers of MgO:LN can be supplied with attractive volume discounts. Other orientations or increased wafer size (100mm) can be supplied on demand.

Part #	Orientation/ Thickness	Ø
MgO:LN		
97-03044-01	Z-axis / 0.5 mm	76.2 mm
97-03044-02	Z-axis / 1.0 mm	76.2 mm
SLT		
97-03022-02	Z-axis / 1.0 mm	76.2 mm

REFERENCES

1. F. Jermann, M. Simon, and t. E. Kratzig, *J. Opt. Soc. Am. B* **12**, 2066 (1995).
2. J. L. Nightingale, W. J. Silva, G. E. Reade, A. Rybicki, W. J. Kozlovsky, and R. L. Byer, *Proc. SPIE* **681**, 20-24 (1986).
3. D. A. Bryan, R. Gerson, and H. E. Tomaschke, *Appl. Phys. Lett.* **44**, 847 (1984).
4. D. H. Jundt, M. C. C. Kajiyama, D. Djukic, and M. Falk, *Journal of Crystal Growth*, In Press, Corrected Proof (2009).
5. Y. Furukawa, K. Kitamura et.al., *Applied Physics Letters* **77**, 2494-6 (2000).
6. S. I. Bae, J. Ichikawa, K. Shimamura, H. Onodera, and T. Fukuda, *Journal of Crystal Growth* **180**, 94-100 (1997).
7. D. S. Hum, R. K. Route, G. D. Miller, V. Kondilenko, A. Alexandrovski, J. Huang, K. Urbaneck, R. L. Byer, and M. M. Fejer, *Journal of Applied Physics* **101** (2007).
8. Y. Furukawa, K. Kitamura, A. Alexandrovski, R. K. Route, M. M. Fejer, and G. Foulon, *Applied Physics Letters* **78**, 1970-2 (2001).
9. M. Falk, T. Woike, and K. Buse, *Applied Physics Letters* **90**, 251912-3 (2007).
10. I. Breunig, M. Falk, B. Knabe, R. Sowade, K. Buse, P. Rabiei, and D. H. Jundt, *Appl Phys. Lett.* **91**, 221110 (2007).